



Supporting Information

© Wiley-VCH 2009

69451 Weinheim, Germany

---

# **Towards Photoconductive Covalent Organic Framework: Self-Condensed Arene Cubes with Eclipsed Order of 2D Polypyrene Sheets for Prominent Photocurrent Generation**

Shun Wan, Jia Guo, Jangbae Kim, Hyotcherl Ihee, and Donglin Jiang\*

---

## **Section 1. Materials and Methods**

### **Section 2. Synthesis**

### **Section 3. FT IR Spectral Profile**

### **Section 4. Simulation and Calculation of Crystal Lattice Packing**

### **Section 5. Fluorescence Excitation and Diffuse Reflectance UV- NIR Spectral Profiles**

### **Section 6. Electric Conductivity and Photoconductivity of PDBA**

### **Section 7. Photoconductivity of TP-COF**

### **Section 8. Supporting References**

## **Section 1. Materials and Methods**

THF was distilled over benzophenone ketyl under Ar before use. Cyclohexane was distilled under Ar before use. Pyrene, bispinacolatodiboron, anhydrous 1,4-dioxane (99.8%) and anhydrous acetone (99.8%) were purchased from Wako Chemicals. Mesitylene (98%) were purchased from TCI. 4,4'-di-*tert*-butyl-2,2'-bipyridine was purchased from Aldrich. Sodium periodate and hydrochloric acid were purchased from Kanto Co. Ltd. Methoxy(cyclooctadiene)iridium(I) dimer was purchased from Alfa Aesar Chemicals. Silica gel Wakogel C-300HG was used for column chromatography. Deuterated solvents for NMR measurements were obtained from Cambridge Isotope Laboratories, Inc. Pyrene-2,7-diboronic ester<sup>1</sup> and PDBA (Ref. 9) were prepared according to reported methods.

$^1\text{H}$  and  $^{13}\text{C}$  NMR spectra were recorded on JEOL models JNM-LA400 or JNM-LA500 NMR spectrometers, where chemical shifts ( $\delta$  in ppm) were determined with a residual proton of the solvent as standard. Infrared (IR) spectra were recorded on a JASCO model FT IR-6100 Fourier transform infrared spectrometer. UV-Vis-IR diffuse reflectance spectrum (Kubelka-Munk spectrum) was recorded on a JASCO model V-670 spectrophotometer equipped with integration sphere model IJN-727. Fluorescence spectroscopy was recorded on a JASCO model FP-6600 spectrofluorometer. Matrix-assisted laser desorption ionization time-of-flight mass (MALDI-TOF-MS) spectra were recorded on an Applied Biosystems BioSpectrometry model Voyager-DE-STR spectrometer in reflector or linear mode using 9-nitroanthracene or dithranol as matrix. Field emission scanning electron microscopy (FE SEM) was performed on a JEOL model JSM-6700 FE-SEM operating at an accelerating voltage of 1.5 or 5.0 kV. The sample was prepared by drop-casting an acetone suspension onto mica substrate and then coated with gold. Transmission Electron Microscope (TEM) images were obtained on a JEOL model JEM-3200 microscope. The sample was prepared by drop-casting an acetone suspension of TP-COF onto a copper grid. Powder X-ray diffraction (PXRD) data were recorded on a Rigaku model RINT Ultima III diffractometer by depositing powder on glass substrate, from  $2\theta = 1.5^\circ$  up to  $60^\circ$  with  $0.02^\circ$  increment at  $25^\circ\text{C}$ .

Nitrogen sorption isotherms were measured at  $77\text{ K}$  with a Bel Japan Inc. model BELSORP-mini II analyzer. Before measurement, the samples were degassed in vacuum at  $200^\circ\text{C}$  for more than 6h. The Brunauer-Emmett-Teller (BET) method was utilized to calculate the specific surface areas. By using non-local density functional theory (NLDF) model, the pore size was derived from the sorption curve.

Electrical measurements were carried out at  $25^\circ\text{C}$  in air on PPy-COF or  $\text{I}_2$ -doped PPy-COF between  $10\text{-}\mu\text{m}$  width Pt electrodes by a two-probe method using a Keithley model 2635 sourcemeter. PPy-COF was homogeneously dispersed in acetone and casted onto the electrode to give a film. For  $\text{I}_2$  doping, the PPy-COF electrode was kept in an  $\text{I}_2$  atmosphere for 1h before measurement. As for the fabrication of devices for photoirradiation, PPy-COF was dispersed in PMMA/ $\text{CHCl}_3$  (PPy-COF/PMMA = 50/50 wt%) to cast a thin film on Al electrode and Au electrode (30-nm thickness) was vapor deposited on the top of the film, to give a sandwich-type electrode gaps. PMMA was utilized as a glue to disperse PPy-COF

homogenously since PMMA is free of any absorption in the irradiation wavelength region and has been widely utilized as a standard glue for polymer samples in photo-generated carrier conductivity measurement.<sup>2</sup> The film thickness was about 100  $\mu\text{m}$  as estimated by FE SEM measurement. A Xenon light source of Asahi Spectra MAX-301 model was utilized for the irradiation on the top of Au electrode. Due to the difference in electrode configurations, the observed currents are not comparable for those using Pt gap electrodes and sandwich-type Al/Au electrodes.

Geometry optimization of the unit pore structure was performed at PM3 level by using the Gaussian 03 program package (Revision C.02)<sup>3</sup> to give the pore size of 1.73 nm in diameter. Geometry optimization of the repeating unit was performed at B3LYP/6-31G(d) level by using the Gaussian 03 program package in order to make unit cell structure. The final molecular structure in a hexagonal unit cell was prepared by using geometrical parameters from the optimized structure and the pore size of 1.73 nm was retained in the final structure. Molecular modeling and Pawley refinement were carried out using Reflex, a software package for crystal determination from PXRD pattern, implemented in MS ver 4.2 (Accelrys Inc.).<sup>4</sup> Unit cell dimension was first manually determined from the observed PXRD peak positions by using hexagonal arrangement. We performed Pawley refinement to optimize the lattice parameters iteratively until the  $R_{\text{WP}}$  value converges. The refinement indicates a hexagonal crystal system with a unit cell of  $a = b = 22.16295(838) \text{ \AA}$  and  $c = 3.42066(165) \text{ \AA}$ . The pseudo-Voigt profile function was used for whole profile fitting and Berrar-Baldinozzi function was used for asymmetry correction during the refinement processes. The final  $R_{\text{WP}}$  and  $R_{\text{p}}$  values were 8.10% and 5.64%, respectively. Simulated PXRD patterns were calculated from the refined unit cell and compared with the experimentally observed patterns. This structure could have two distinct arrangements: (1) a staggered AB type arrangement with graphite-like packing, where three-connected vertices lie over the center of the six-membered rings of neighboring layers; (2) an eclipsed AA type arrangement, where all atoms in an each layer of the framework lie exactly over one another. The AA type arrangement was constructed in space group  $P6/mmm$  symmetry (space group number 191) and the AB type arrangement was constructed in space group  $P63/mmc$  symmetry (space group number 194). The atoms are placed on the special position to form the 2D framework

where all bond lengths and angles are taken from the optimized geometrical parameters calculated at B3LYP/6-31G(d) to maintain reasonable values. After comparing each simulated pattern with experimentally observed pattern, only the simulated pattern from the eclipsed AA type arrangement shows good agreement with the observed PXRD pattern.

## Section 2. Synthesis

All reactions were performed under argon using Schlenk line technique.

**PPy-COF:** A 1,4-dioxane/mesitylene (2.5 mL/2.5 mL) mixture of PDBA (25.0 mg, 0.345 mmol) in a 10-mL pyrex tube was degassed by three freeze-pump-thaw cycles, then the tube was sealed, kept in autoclave and heated at 120 °C for 2 days. The precipitate was collected by centrifugation, washed with anhydrous acetone and dried at 150 °C under vacuum to give PPy-COF (22 mg) as pale yellow powder in 88% yield.

## Section 3. FT IR Spectral Profile

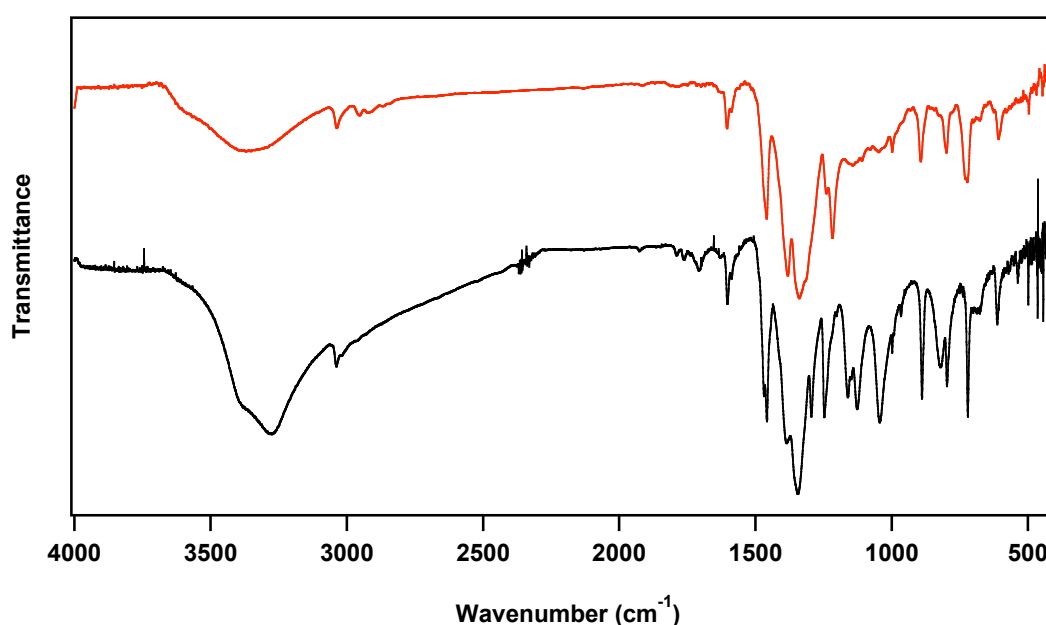


**Figure S2.** FT IR spectra of PDBA (black curve) and PPy-COF (red curve).

**Table S1:** Peak assignments for FT-IR spectrum of PPy-COF.

Peak (cm <sup>-1</sup> )	Assignment and Notes
3369.51 (m)	O–H stretch from the end B(OH) <sub>2</sub> or OH groups of PPy-COF.
3036.37 (w)	Aromatic C–H stretch from pyrene unit.
2953.45 (w)	C–H stretching from mesitylene guest molecule.
2922.11 (w)	
2867.15 (w)	
1604.00 (w)	C=C stretch for fused aromatics.
1588.57 (m)	C=C vibrational mode of phenyl ring of pyrene unit.

1458.89 (m)	C=C vibrational modes for p-substituted pyrene unit.
1380.78 (s)	B–O stretch, characteristic band for boroxoles.
1339.32 (s)	B–O stretch, characteristic band for boroxoles.
1316.66 (s)	C–C stretch, characteristic for boroxoles.
1239.52 (m)	C–O stretch, characteristic for boroxoles.
1143.58 (w)	C–H in-plane bending modes.
1109.35 (w)	
1047.64 (m)	B–C stretch.
998.46 (m)	C–H out-of-plane bending modes for <i>p</i> -substituted aromatic rings.
893.36 (m)	
798.39 (m)	C–H out-of-plane bending modes
721.73 (m)	
700.03 (w)	
609.88 (w)	

## Section 4. Simulation and Calculation of Crystal Lattice Packing

### 1. Crystal Data

Formula	$C_{48}H_{24}B_6O_6$
Formula weight	761.58
Crystal system	Hexagonal
Space group	$P6/mmm$ (No.191)
Unit cell dimensions	$a = b = 22.16295(838) \text{ \AA}$ $c = 3.42066(165) \text{ \AA}$
Cell volume	$1455.12 \text{ \AA}^3$
Density calculated	$0.869 \text{ g/cm}^3$

### 2. Atomic Coordinate

Atom	Wyck.	x	y	z
C1	$12q$	0.14521	0.62588	1/2
C2	$12q$	0.07328	0.59117	1/2
C3	$12q$	0.03489	0.62661	1/2
H4	$12q$	0.17408	0.68527	1/2
H5	$12q$	0.06339	0.68600	1/2
B6	$6m$	0.26177	0.63088	1/2
C7	$6m$	0.18206	0.59103	1/2
C8	$6m$	0.03650	0.51825	1/2
C9	$6m$	0.29791	0.59581	1/2

### 3. Simulation of PXRD Pattern and Crystal Packing

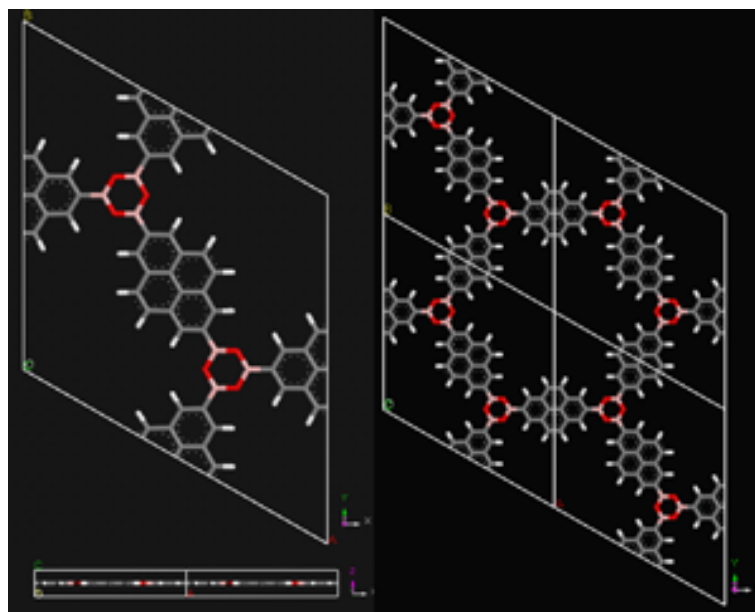
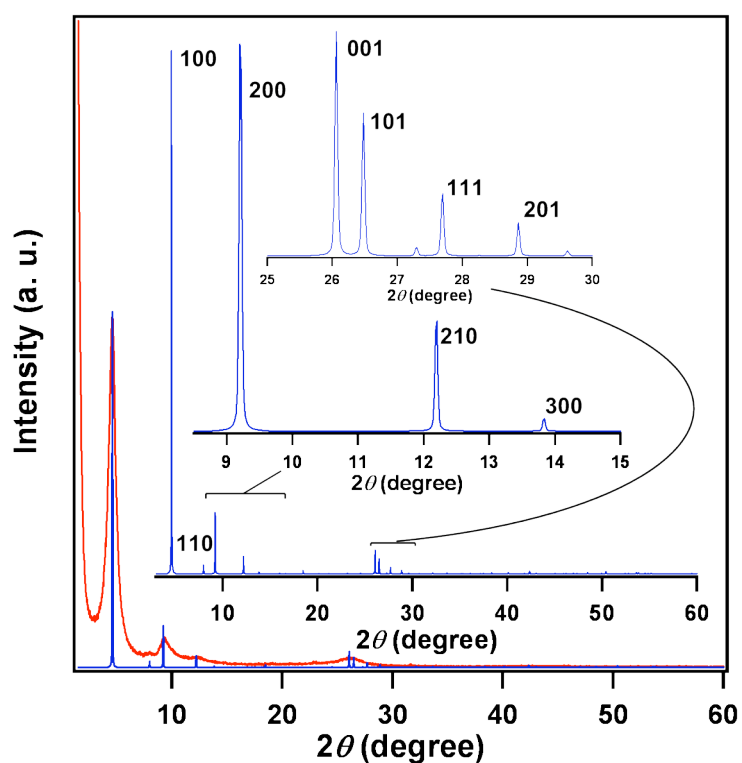


**Figure S3.** PXRD pattern of PPy-COF and simulation of crystal lattice packing in the eclipsed form. In the upper figure, the red curve represents the experimental PXRD pattern and the blue pattern is calculated from the eclipsed crystal packing (Crystal space group  $P6/mmm$ ; No. 191). The calculated pattern simulates the experimental data well. The insets show the assignment of PXRD signals. The lower figure shows the eclipsed crystal lattice packing of PPy-COF. The pore size is 1.73 nm in diameter in the defined structure.

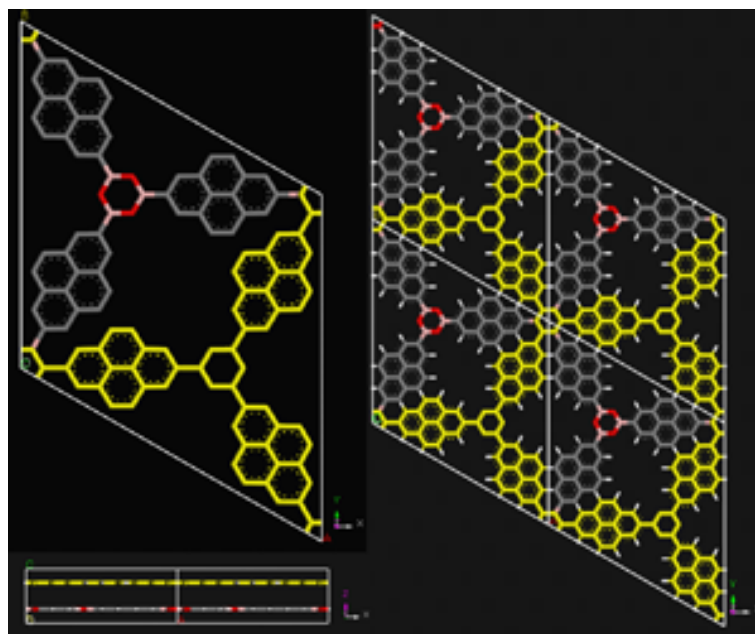
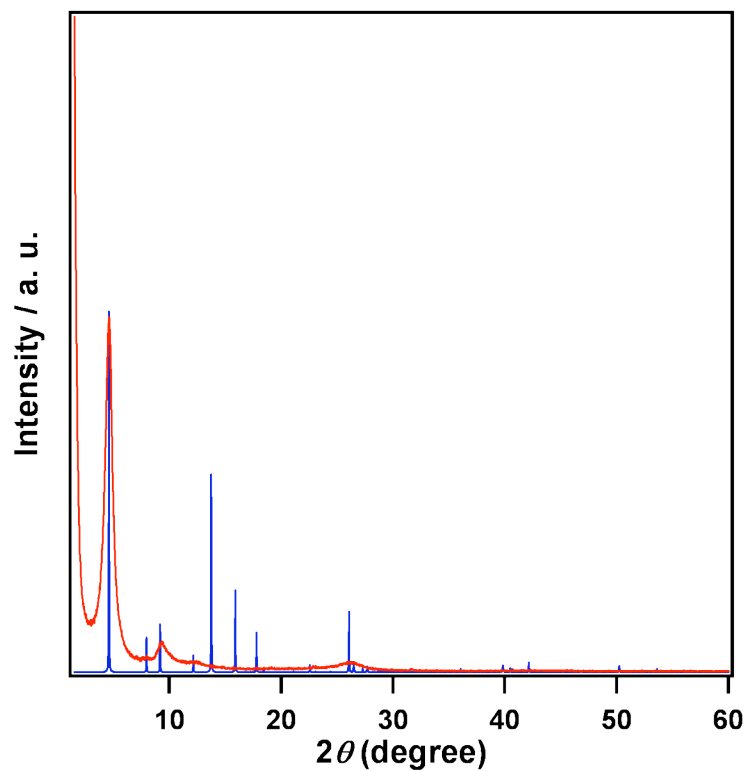


**Figure S4.** PXRD pattern of PPy-COF and simulation of crystal lattice packing in the staggered form. In the upper figure, the red curve represents the experimental PXRD pattern and the blue pattern is calculated from the staggered crystal packing (Crystal space group  $P63/mmc$ ; No. 194). The simulated pattern does not fit the experimental data at all. The lower figure shows the staggered crystal lattice packing. In this case, the pore is covered and the pore size is significantly smaller than the experimental one.

## Section 5. Fluorescence Excitation and Diffuse Reflectance UV-NIR Spectral Profiles

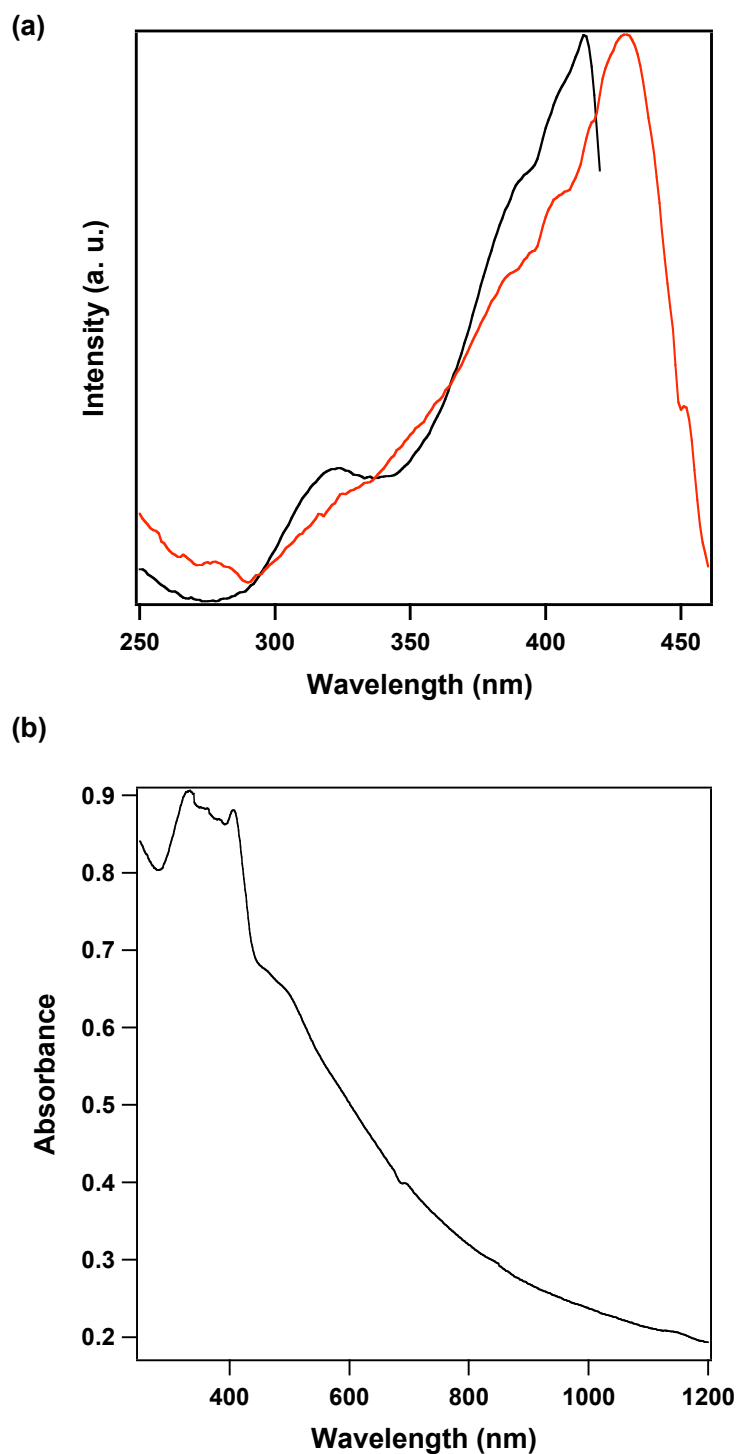


**Figure S5.** (a) Normalized fluorescence excitation spectra of PDBA (black curve) and PPy-COF (red curve). (b) Diffuse reflectance UV-VIS-NIR spectrum of PPy-COF.

## Section 6. Electric Conductivity and Photoconductivity of PDBA

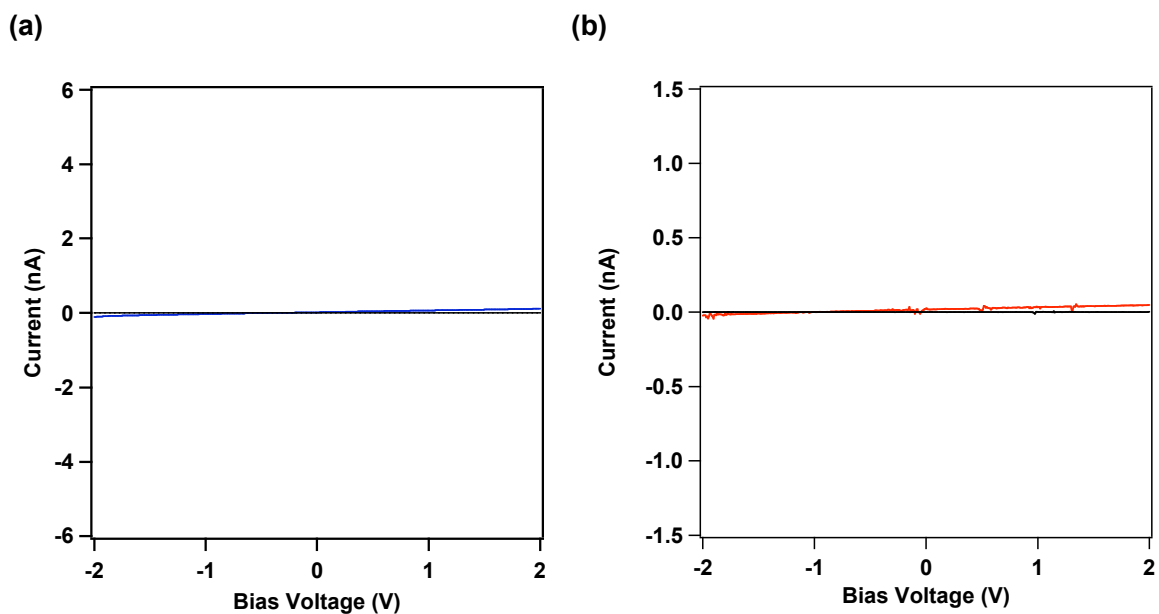


**Figure S6.** a) Electric conductivity of PDBA (blue curve) on 10- $\mu\text{m}$  width Pt gap electrodes at 25 °C (black curve: electrodes only). b) Photoconductivity of PDBA between Al/Au sandwich type electrodes upon irradiation with visible light (red curve).

## Section 7. Photoconductivity of TP-COF

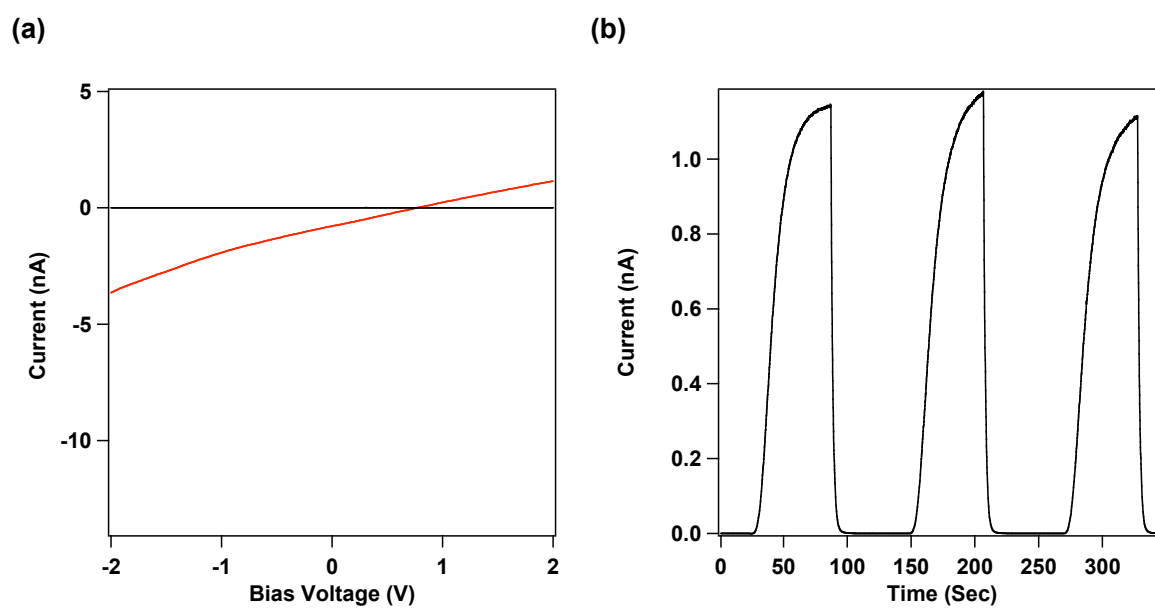


**Figure S7.** a) I-V profile of TP-COF between sandwich-type Al/Au electrodes (black curve: without light irradiation; red curve: upon light irradiation). (b) Photocurrent when light is turned on or off. TP-COF shows a low photocurrent (1.14 nA at 2 V bias voltage) and a small on/off ratio of about  $2.0 \times 10^4$ , which is only one-fourth that of PPy-COF, under otherwise identical conditions.

## Section 8. Supporting References

- S1. Coventry, D. N.; Batsanov, A. S.; Goeta, A. E.; Howard, J. A. K.; Marder, T. B.; and Perutz, R. N. *Chem. Commun.* 2005, 2172.
- S2. Acharya, A.; Seki, S.; Koizumi, Y.; Saeki, A.; and Tagawa, S. *J. Phys. Chem. B* 2005, **109**, 20174.
- S3. Gaussian 03, Revision C.02, Frisch, M. J.; Trucks, G. W.; Schlegel, H. B.; Scuseria, G. E.; Robb, M. A.; Cheeseman, J. R.; Montgomery, Jr., J. A.; Vreven, T.; Kudin, K. N.; Burant, J. C.; Millam, J. M.; Iyengar, S. S.; Tomasi, J.; Barone, V.; Mennucci, B.; Cossi, M.; Scalmani, G.; Rega, N.; Petersson, G. A.; Nakatsuji, H.; Hada, M.; Ehara, M.; Toyota, K.; Fukuda, R.; Hasegawa, J.; Ishida, M.; Nakajima, T.; Honda, Y.; Kitao, O.; Nakai, H.; Klene, M.; Li, X.; Knox, J. E.; Hratchian, H. P.; Cross, J. B.; Bakken, V.; Adamo, C.; Jaramillo, J.; Gomperts, R.; Stratmann, R. E.; Yazyev, O.; Austin, A. J.; Cammi, R.; Pomelli, C.; Ochterski, J. W.; Ayala, P. Y.; Morokuma, K.; Voth, G. A.; Salvador, P.; Dannenberg, J. J.; Zakrzewski, V. G.; Dapprich, S.; Daniels, A. D.; Strain, M. C.; Farkas, O.; Malick, D. K.; Rabuck, A. D.; Raghavachari, K.; Foresman, J. B.; Ortiz, J. V.; Cui, Q.; Baboul, A. G.; Clifford, S.; Cioslowski, J.; Stefanov, B. B.; Liu, G.; Liashenko, A.; Piskorz, P.; Komaromi, I.; Martin, R. L.; Fox, D. J.; Keith, T.; Al-Laham, M. A.; Peng, C. Y.; Nanayakkara, A.; Challacombe, M.; Gill, P. M. W.; Johnson, B.; Chen, W.; Wong, M. W.; Gonzalez, C.; and Pople, J. A.; Gaussian, Inc., Wallingford CT, 2004.
- S4. Accelrys, Material Studio Release Notes, Release 4.2, Accelrys Software, San Diego 2006.